Core Design and Safety Studies for a Small Modular Fast Reactor

W. S. Yang, J. E. Cahalan, and F. E. Dunn
Argonne National Laboratory, 9700 South Cass Avenue, Argonne, IL 60439, U.S.A.

Abstract

The paper describes the core design and performance characteristics and the safety analysis results for a 50 MWe small modular fast reactor design that was developed jointly by ANL, CEA, and JNC as an international collaborative effort. The main goal in the core design was to achieve a 30-year lifetime with no refueling. In order to minimize the burnup reactivity swing, metal fuel with a high heavy metal volume fraction was selected. To enhance the proliferation resistance and actinide transmutation, all the transuranic (TRU) elements recovered from light water reactor spent fuel were used in a ternary alloy form of U-TRU-10Zr. A 125 MWt core design was developed, for which the burnup reactivity swing was only 1.6$ over the 30-year core lifetime. The average discharge burnup was 87 MWd/kg, and the maximum sodium void worth was 4.65$. The evaluated reactivity coefficients provided sufficient negative feedbacks. Shutdown margins of control systems were confirmed. Steady-state thermal-hydraulic analysis results showed that peak 2σ cladding inner-wall and fuel centerline temperatures were less than design limits with sufficient margins. Detailed transient analyses for the total loss of power to reactor and intermediate coolant pumps showed that no fuel damage or cladding failure would occur, even when multiple safety systems were assumed to malfunction.

KEYWORDS: core design and safety studies, sodium cooled fast reactor, long-life core, transuranic metal fuel.

1. Introduction

A joint study among Argonne National Laboratory (ANL), Commissariat à l'Energie Atomique (CEA), and Japan Nuclear Cycle Development Institute (JNC) was performed to develop a sodium-cooled, small modular fast reactor (SMFR). In this international collaborative effort, a 50 MWe SMFR design was developed in 2005 for a specific niche application to small grid systems, where the industrial infrastructure is under-developed and the unit cost of electricity generation is very high with conventional technologies. Various innovative design features were incorporated into the SMFR design including a metallic fueled core with 30-year lifetime, inherent passive safety characteristics, simplified reactor system for modular construction and transportability, and a supercritical CO_2 Brayton cycle power conversion system. The primary system is configured as a typical pool-type arrangement, with the reactor core, primary pumps, intermediate heat exchangers, and direct reactor auxiliary cooling system (DRACS) heat exchangers all contained within the reactor vessel. [1,2] In this paper, the core design and performance characteristics of the SMFR design are described along with safety analysis results.

The main goal in core design was to achieve a 30-year lifetime with no refueling. A near-zero burnup reactivity swing is required to achieve this design goal without an excessive reactivity control requirement or an unnecessary decrease in power density. This necessitates an internal conversion ratio slightly larger than 1.0, which in turn requires the fertile isotope fraction high enough (i.e., low fissile enrichment). To maintain the core criticality with low enrichment fuel, dense fuel loading is necessary. For a dense fuel-loading design, metal fuel with a high fuel volume fraction was selected. To attain a high fuel volume fraction without increasing the core pressure drop, a large diameter pin design was employed. An enrichment zoning strategy was adopted to flatten the power distribution. To enhance the proliferation resistance and actinide transmutation, all the transuranic (TRU) elements recovered from light water reactor (LWR) spent fuel with 50 MWd/kg burnup were used in a ternary alloy form of U-TRU-10Zr. Low-swelling ferritic stainless steel (HT-9) cladding was selected because of high fluence expected for a long life core. Three-zone fuel enrichment (i.e., TRU fractions) was used to reduce the radial power peaking and to enhance internal conversion over 30-year lifetime.

A 125 MWt core design was developed through trade-off and optimization studies, focused on the minimization of reactivity swing and flattening of radial power distribution over the 30-year core lifetime. The principal design variables investigated include the fuel pin diameter, assembly size, active core height, core configuration, material volume fractions, enrichment zoning and ratios, and lower reflector and fission-gas plenum lengths. Key thermal-hydraulic and materials related design constraints include the fuel smeared density of 75%, peak 2σ cladding inner wall temperature less than 650 °C, peak 2σ fuel centerline temperature less than the melting temperature of ternary metal fuel, and maximum irradiation damage of in-vessel structures less than 5 dpa. In order to achieve a 30-year fuel lifetime within a fast fluence limit of HT-9 cladding, the core power density was reduced significantly relative to conventional sodium-cooled fast reactors. The coolant inlet and bulk outlet temperatures were 355 °C and 510 °C, respectively. Flow orificing was provided within the assembly inlet modules, and individual assembly orifices were determined such that the peak 2σ cladding mid-wall temperatures at the beginning of life (BOL) and end of life (EOL) are equal.

In Section 2, the physics and safety models used in the design calculations are detailed. The core design and performance characteristics are discussed in Section 3. In Section 4 the modeling assumptions used in the safety study and a summary of the base case condition are given. Finally, conclusions are drawn from both the reactor physics and safety analysis.

2. Computational Models and Methods

The ANL suite of fast reactor analysis codes was used to evaluate core performance parameters and reactivity coefficients. Fuel cycle analyses were performed with the DIF3D/REBUS-3 code system [3,4]. The region-dependent 21-group cross section set generated for the metal fuel core with the ETOE-2/MC2-2/SDX code system [5-7] based on ENDF/B-V.2 was used. Equilibrium and non-equilibrium cycle analyses were performed using 3-dimensional hexagonal-z geometry models with individual assemblies. A 90% capacity factor was assumed. Irradiation swelling of metal fuel and material thermal expansion at operating condition were modeled by adjusting the hexagonal pitch, axial meshes, and the fuel and structure volume fractions appropriately and by displacing the bond sodium into lower part of plenum. Block nuclide depletion was performed by

dividing each fuel assembly into five axial depletion zones. For flux calculations, the hexagonal-z nodal diffusion theory option of DIF3D [8] was mainly employed, and VARIANT transport theory option [9] was used for comparison. The TRU fraction in fuel was first determined from the equilibrium cycle analysis such that k-effective at BOL is 1.0, and detailed non-equilibrium cycle analyses with refined burn time intervals were performed using this TRU fraction.

Reactivity coefficients and kinetics parameters were calculated for the BOL, MOL (mid of life), and EOL core configurations. The MOL is the time point when the excess reactivity attains its maximum value over the core lifetime. The coolant, fuel, and structure density coefficients and the coolant void coefficient were determined using the VARI3D perturbation code [10]; the linear perturbation theory option was used for density coefficients, while the exact perturbation theory option was employed for the coolant void coefficient. The effective delayed neutron fraction and prompt neutron lifetime were also calculated using the VARI3D code. The radial and axial expansion coefficients and the control rod worth were determined by direct eigenvalue differences of the base and perturbed conditions using the DIF3D code. Calculations for in-vessel structure fast fluence and displacement per atom (dpa) were performed using the TWODANT transport code [11]. Neutron fluxes for BOL and EOL configurations were determined in RZ geometry with S_{16} angular discretization. The fast fluence and dpa were estimated using the average values of BOL and EOL fluxes and 28-group dpa cross sections generated using the NJOY code [12] based on ENDF-VI.

For steady-state thermal-hydraulic analyses, coupled neutron and gamma heating calculations were performed using the triangular-z finite difference option of the DIF3D code; the gamma source distribution was determined using the GAMSOR code [13]. The sub-channel analysis code SE2-ANL [14] was employed for whole core temperature calculations. Sodium flow was distributed to the assemblies with the overall goal of equalizing pin cladding damage accrual and thus pin reliability. Assembly flow rates were determined such that the peak 2σ cladding mid-wall temperatures of individual fuel assemblies were equalized over the core lifetime. Hot channel factors were included in temperature predictions to account for core design, analysis, fabrication and operational uncertainties and variations. Hot channel factors for PRISM design [15] were used for 2σ cladding and fuel temperature calculations.

The safety analyses were performed using the SAS4A/SASSYS-1 code [16]. The thermal-hydraulic performance of the reactor core was analyzed with a geometric model consisting of single-pin channels. In this multi-channel whole-core model, each channel represents a single, average pin in a subassembly, and several subassemblies are grouped together, so that a single channel may represent all the pins in a number of subassemblies. The coolant flow and heat transfer in the primary and intermediate sodium systems and in the emergency decay heat removal system were modeled with a network of volumes and components connected by flow paths. Components in this model included the inlet and outlet plenums, pipes, electromagnetic pumps, heat exchangers, and DRACSs. A point kinetics model was employed to calculate the reactor fission power response to the transient reactivity state. At any time, the net reactivity is the sum of a number of individual reactivity feedbacks that are determined by the transient thermal, hydraulic, mechanical, and neutronics state of the reactor. The feedback reactivities considered in this study are fuel Doppler, coolant density, fuel and cladding axial thermal expansion, radial core expansion, and control rod driveline thermal expansion. A decay heat model is integrated with the point kinetics model for the fission power to track shutdown events in sub-critical conditions.

3. Core Design and Performance Characteristics

As shown in Fig. 1, the SMFR core is composed of 48 fuel assemblies and 7 control assemblies surrounded by 30 reflector assemblies and 36 shield assemblies. Three fuel enrichment zones are used to flatten the radial power distribution and to enhance the internal conversion. The fuel assembly design parameters and the core performance characteristics are summarized in Table 1. The fuel is U-TRU-10%Zr metallic alloy, and the TRU fractions of heavy metal in the inner, middle, and outer cores are 10.3, 14.9, and 16.0 %, respectively. The total heavy metal and TRU inventories are 13,849 kg and 1,960 kg, respectively. The burnup reactivity swing is only 1.6$ over the 30-year core lifetime. The excess reactivity initially decreases slightly due to axial expansion of metal fuel, and then increases gradually due to fissile material buildup in the inner core. After

Figure 1. SMFR Core Layout

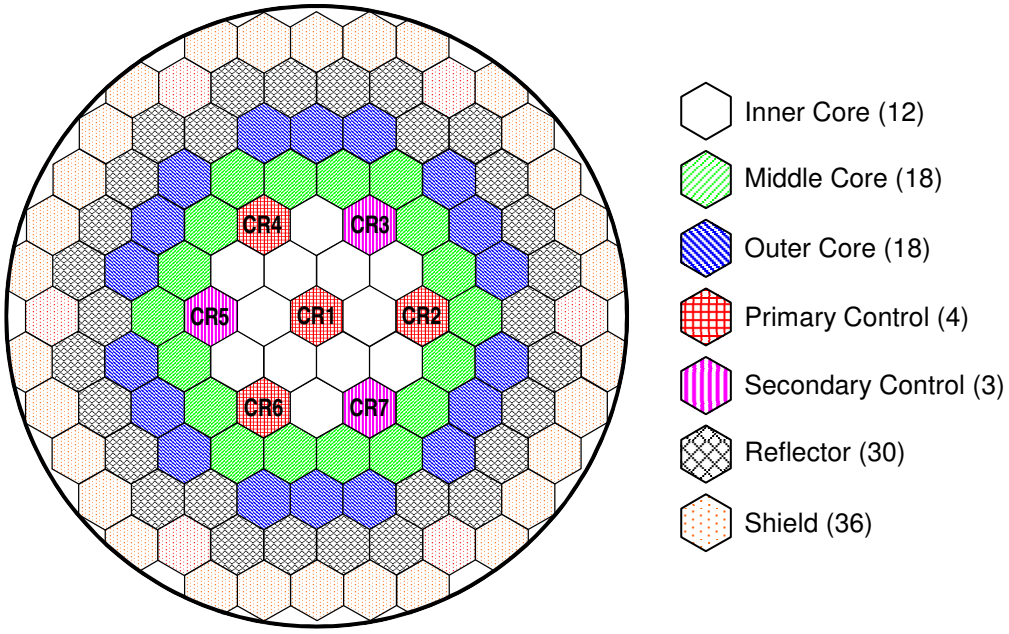

Table 1. Fuel Assembly Design and Core Performance Characteristics

Number of pins per assembly	217	Initial heavy metal loading (kg)	13,840
Assembly pitch (cm)	22.165	Initial TRU loading (kg)	1,960
Fuel material	U-TRU-10Zr	Specific power (kW/kg)	9.03
Bond material	Sodium	Power density (W/cm^3)	56.5
Cladding material	HT-9	Reactivity swing ($)	1.6
Pin diameter (cm)	1.750	Conversion ratio	1.005
Pin pitch-to-diameter ratio	1.064	Power peaking factor, BOL/EOL	1.59/1.61
Fuel smeared density (%)	75	Average burnup (MWd/kg)	86.7
Active core height (cm)	100	Peak burnup (MWd/kg)	133.2
Fission gas plenum height (cm)	150	Peak fast fluence (10^{23} n/cm^2)	5.10

reaching its maximum around 17 effective full power years (EFPY), it decreases monotonically because of the insufficient conversion resulting from reduced fertile material. The average conversion ratio is 1.005. The average burnup is 87 MWd/kg, and the peak burnup is 133 MWd/kg. These burnups are similar to those of conventional fast reactors, but they are achieved over the 30-year fuel residence time with a reduced power density by a factor of ~5, which increases the construction cost per unit power output. It is also noted that the peak fast fluence is ~25% higher than the typical limit used for HT-9 cladding. It might be necessary to reduce the power density further or decrease the targeted core lifetime. To ensure the fuel integrity over the 30-year lifetime, detailed fuel performance analyses need to be performed.

Table 2 presents the calculated neutron kinetics parameters and reactivity coefficients. The delayed neutron fraction decreases slightly with increasing burnup. The prompt neutron lifetime is about 220 ns throughout the core lifetime. The largest sodium void worth occurs at EOL and is 4.65$. The Doppler coefficients are about -0.07 cents/°C and -0.05 cents/°C for flooded and voided sodium cases, respectively. The voided Doppler coefficient is slightly less negative due to hardened neutron spectrum. For uniform expansion, the radial expansion coefficient is about -0.20 cents/°C and the axial expansion coefficient is -0.07 cents/°C.

Table 2. Neutron Kinetics Parameters and Reactivity Feedback Coefficients

	BOL	MOL	EOL
Delayed Neutron Fraction	0.0039	0.0036	0.0035
Prompt Neutron Lifetime (μs)	0.219	0.216	0.216
Sodium Void Worth ($)	3.83	4.46	4.65
Sodium Density Coefficient (cents/°C)	0.09	0.11	0.11
Fuel Density Coefficient (cents/°C)	-0.51	-0.53	-0.55
Structure Density Coefficient (cents/°C)	0.03	0.04	0.04
Radial Expansion Coefficient (cents/°C)	-0.19	-0.20	-0.20
Axial Expansion Coefficient (cents/°C)	-0.07	-0.07	-0.07
Doppler Coefficient (cents/°C)	-0.07	-0.07	-0.06
Voided Doppler Coefficient (cents/°C)	-0.05	-0.05	-0.05

As shown in Fig. 1, two independent sets of control rod assemblies are employed for reactivity control and reactor shutdown: a primary and a secondary system. The primary system is required to bring the reactor from any operating condition to cold sub-critical at the refueling temperature with the most reactive control assembly stuck at the full power operating position. The secondary system is required to shut down the reactor from any operating condition to the hot standby condition, also with the most reactive assembly inoperative. The primary system also serves to compensate for the reactivity effects of the fuel burnup and axial growth of metal fuel. The reactivity associated with uncertainties in criticality and fissile loading is accommodated by the primary control system. The estimated reactivity addition by the accidental withdrawal of the most reactive control assembly is 0.18$, 0.51$, and 0.16$ at BOL, MOL, and EOL, respectively. The calculated minimum shutdown margins of primary and secondary systems are 4.12$ and 3.97$, respectively.

In-vessel structure shielding appeared to be adequate. The calculated peak irradiation damage

for the 30-year core lifetime is about 1.5 dpa for the grid plate and less than 0.5 dpa for core barrel. A significant power shift over the 30-year lifetime was observed; high power region is moved from the outer core at BOL to the inner core at EOL due to the relatively high conversion ratio of the inner core. However, by appropriate coolant flow allocation, all the design constraints are met with enough margins. The peak 2σ cladding inner wall temperature is 632 °C, which is lower than the fuel-clad eutectic temperature (650 °C) by ~18 °C. The peak 2σ fuel centerline temperature is lower than fuel melting temperature by ~300 °C. The coolant outlet temperature from an assembly is not different more than 20°C from average temperature of six surrounding assemblies at both BOL and EOL.

4. Safety Analysis

One of the primary goals in the SMFR design has been to provide not only the customary safety margins in design basis events, but also to deliver superior safety performance in beyond design basis events involving multiple equipment failures or unplanned operator actions. These characteristics are desirable for all nuclear reactors, but especially in the case of SMFR, which is intended for remote sites and optimized for minimum attention in normal operation and maximum self-protection in upset conditions. Consequently, the preliminary analysis examines the behavior of SMFR in response to an accident initiator that is normally considered to have a low occurrence frequency, but might have severe consequences, especially with failure of engineered safety systems.

The accident initiator examined here is the total loss of normal power to the reactor cooling system while the plant is operating at full rated power. The loss of power is accompanied by a complete failure of the emergency power supply system, resulting in a total loss of power to the reactor and intermediate coolant pumps. It is also assumed that the power generation plant immediately ceases operation, and provides no heat rejection capacity. The sole heat removal path following the loss of forced coolant flow is through the DRACS by natural circulation. This sequence was analyzed for the case without reactor scram. For convenience, it will be called the unprotected loss-of-flow (ULOF). The ULOF accident sequence assumes multiple equipment failures, failures of safety grade protection and cooling systems, and no operator actions. This sequence is an extreme test of the SMFR to provide inherent self-protection against the consequences of the most severe accident initiators.

Figures 2 to 4 show the analysis results of the ULOF accident sequence for the first 500 seconds of transient time after accident initiation, following about 1000 seconds of calculation to establish a steady set of initial conditions. In the ULOF accident, the reactor safety system fails to scram the reactor upon loss of forced coolant flow and normal heat removal, so the accident proceeds from full power. All heat rejection is through the single DRACS loop, with a design heat rejection of 0.5% of full power at nominal conditions. Figure 2 shows the early histories of the total reactor power, the decay heat production, and the coolant flow in channel 3, the hottest assembly. The initial power-to-flow imbalance results in significant transient heating of the reactor, causing the reactivity feedbacks shown in Fig. 3, and the temperature transients shown in Fig. 4.

Initially, the reactor temperatures rise as the coolant flow falls, and inherent reactivity feedbacks reduce the reactor power. At about 30 seconds into the transient, peak cladding temperatures temporarily reach 735 °C for a short period, but the duration is not sufficient to cause significant

Figure 2. ULOF Early Power and Flow History

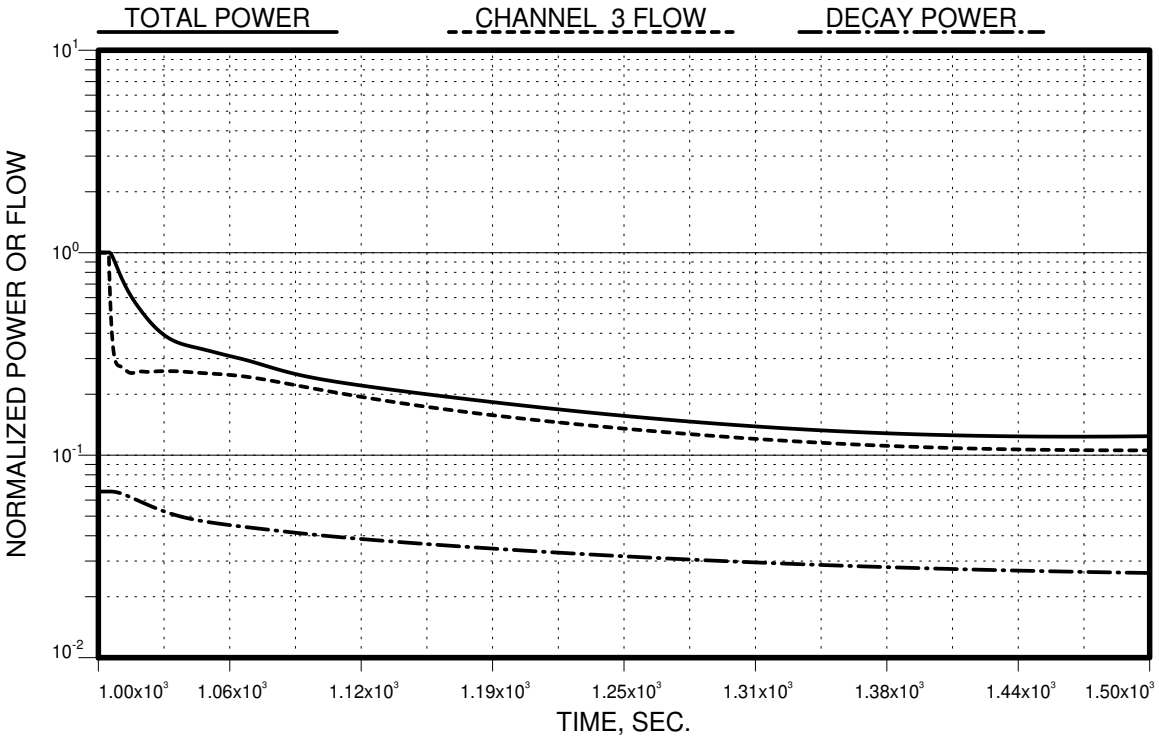

Figure 3. ULOF Early Reactivity History

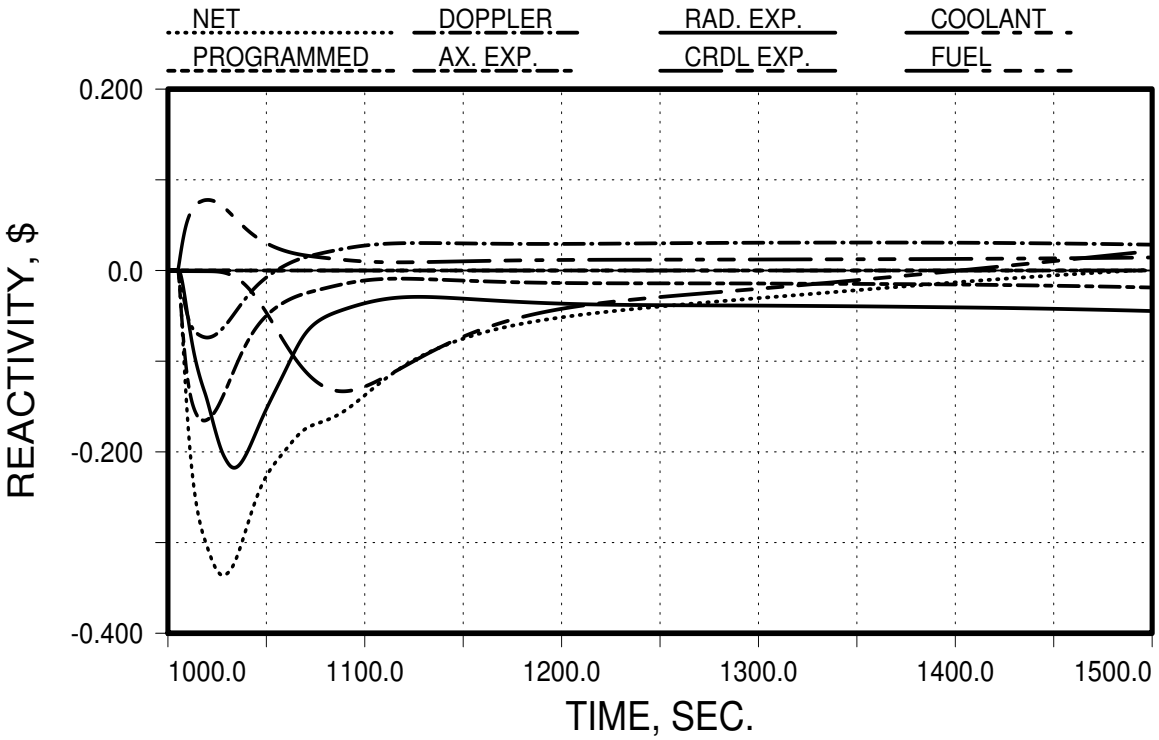

Figure 4. ULOF Early Temperature History

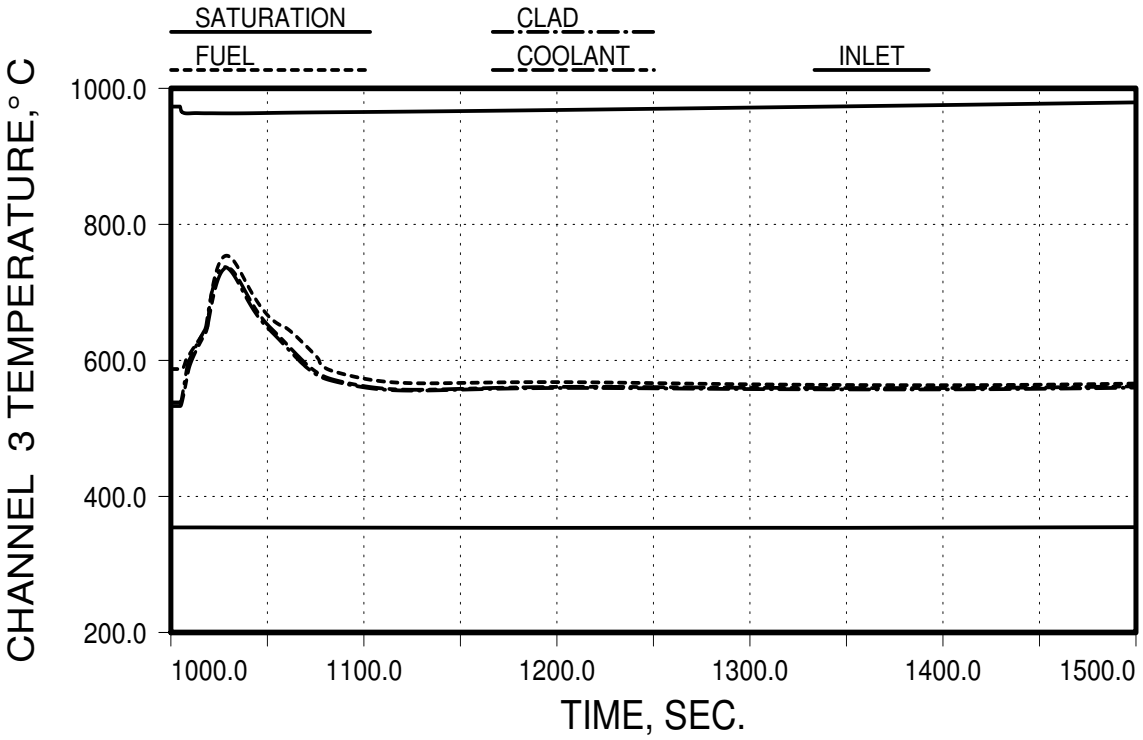

cladding damage or failure. After this time, the power continues to decrease and reactor temperatures fall to approach asymptotic values. The still negative net reactivity rises to zero at 500 seconds, indicating a progression toward equilibrium among the power, the net reactivity, and the temperatures. However, not shown in these graphs is the DRACS heat rejection, which is rising from its original value but not able to remove the power being produced yet. This has the effect of slightly overheating the system, and causing a persistent negative reactivity that extinguishes fission power and maintains reactor heat production at decay heat.

At about 2 hours into the accident, the fission power is extinguished as the total power becomes equal to decay heat production. The net reactivity remains slightly negative at this and subsequent times. Along with the rising inlet temperature, the negative reactivity indicates that the DRACS system heat removal capability is less than the decay heat production, and the system temperature is consequently increasing. With more time, the decay heat production falls, the continued cold pool heating increases the DRACS heat rejection, and eventually, at around five hours into the transient, the DRACS capacity exceeds the decay heat production. This causes a temporary positive net reactivity that rekindles the fission power, and increases the total power (sum of fission and decay heat) to equal the DRACS capacity. For all times following this event, the fission power increases as the decay heat production falls, and the total power remains in equilibrium with the DRACS capacity, at around 0.8%. All system temperatures remain essentially constant after about 5 hours, denoting achievement of an equilibrium condition. In the long term, peak cladding temperatures remain stable at 538 °C, which is nearly identical to the normal operating temperature. Consequently, no fuel damage or cladding failures would occur.

The analysis indicates that the core would survive an unprotected loss-of-flow accident without

pin failures or fuel damage, and that long term equilibrium peak cladding temperatures would remain near the normal operating condition. This very favorable result comes about because of 1) the high thermal conductivity of metallic fuel (low fuel operating temperature, low cold-to-hot reactivity invested at startup), 2) the capability of a sodium-cooled reactor in a pool-type primary system to remove decay heat in natural circulation, and 3) the efficient reactor physics performance permitting an open lattice that further enhances natural circulation capability by reducing the reactor coolant flow pressure drop.

5. Conclusions

The core design and performance characteristics of the 50 MWe SMFR design were discussed along with safety analysis results. The main goal in core design was to achieve a 30-year lifetime with no refueling. To enhance the proliferation resistance and actinide transmutation, all the TRU elements recovered from light water reactor spent fuel were used in a ternary alloy form of U-TRU-10Zr. A 125 MWt core design was developed, of which burnup reactivity swing was only 1.6$ over the 30-year core lifetime. The average conversion ratio was 1.005. The average burnup was 87 MWd/kg and the peak burnup was 133 MWd/kg. The largest sodium void worth occurred at EOL and was 4.65$. It is noted that the core power density was significantly derated compared to conventional sodium-cooled fast reactors. In addition, detailed fuel performance analyses need to be performed to ensure the fuel integrity over the 30-year lifetime.

The reactivity coefficients including Doppler, radial and axial expansion, and coolant, structure and fuel density coefficients were determined to provide sufficient negative feedbacks. The shutdown margins of primary and secondary control systems were also determined to be sufficient; the minimum shutdown margins of primary and secondary systems were 4.12$ and 3.97$, respectively. In-vessel structure shielding appeared to be adequate; peak irradiation damage for the 30-year core lifetime is about 1.5 dpa for the grid plate and less than 0.5 dpa for core barrel. A significant power shift over the 30-year lifetime was observed. However, by appropriate coolant flow allocation, all the design constraints were met with enough margins.

Safety analysis was performed for an unprotected loss-of-flow (ULOF) accident sequence, which is near the end of spectrum of the most pessimistic, challenging, and potentially damaging. The simulation of the accident was performed using analysis techniques and modeling assumptions validated by data from in-pile testing. The computational results showed that for nominal, best-estimate analysis assumptions and input data, the SMFR core would survive an ULOF accident without pin failures or fuel damage, and that long-term equilibrium peak cladding temperatures would remain near the normal operating condition. This very favorable result comes about because of the excellent thermal, hydraulic, and neutronics performance characteristics of a sodium-cooled, metal-fueled reactor design with a primary system pool configuration.

Acknowledgements

The authors wish to thank the following people for their contributions to the SMFR design effort: Chang, Grandy, Farmer, Kamal, Krajtl, Moisseytsev, Monozaki, Sienicki, Park, Tang, Reed, Tzanos and Wiedmeyer of ANL; Allegre, Astegiano, Baque, Cachon, Chenaud, Courouau, Dufour, Klein, Latge, Lo Pinto, Thevenot and Varaine of CEA; and Ando, Chikazawa, Konomura,

Nagamura, Okano, Sakamoto, Sugino and Yamano of JNC. This work was supported by the U.S. Department of Energy under Contract number W-31-109-Eng-38.

References

1) Y. I. Chang, M. Konomura, and P. Lo Pinto, "A Case for Small Modular Fast Reactor," Proc. of GLOBAL 2005: Nuclear Energy Systems for Future Generation and Global Sustainability, Tsukuba, Japan, October 9-13, 2005.
2) Y. I. Chang, et al., "Small Modular Fast Reactor Design Description," ANL-SMFR-1, Argonne National Laboratory (2005).
3) K. L. Derstine, "DIF3D: A Code to Solve One-, Two-, and Three-Dimensional Finite-Difference Diffusion Theory Problems," ANL-82-64, Argonne National Laboratory (1984).
4) B. J. Toppel, "A User's Guide to the REBUS-3 Fuel Cycle Analysis Capability," ANL-83-2, Argonne National Laboratory (1983).
5) "NESC No. 350 ETOE-2 Documentation," National Energy Software Center Note 83-84, August 25, 1983.
6) H. Henryson II, B. J. Toppel, and C. G. Stenberg, "MC2-2: A Code to Calculated Fast Neutron Spectra and Multigroup Cross Sections," ANL-8144, Argonne National Laboratory (1976).
7) W. M. Stacey, Jr., et al, "A New Space-Dependent Fast-Neutron Multigroup Cross Section Preparation Capability," Trans. Am. Nucl. Soc., **15**, 292 (1972).
8) R. D. Lawrence, "The DIF3D Nodal Neutronics Option for Two- and Three-Dimensional Diffusion Theory Calculations in Hexagonal Geometry," ANL-83-1, Argonne National Laboratory (1983).
9) G. Palmiotti, E. E. Lewis, and C. B. Carrico, "VARIANT: VARIational Anisotropic Nodal Transport for Multidimensional Cartesian and Hexagonal Geometry Calculation," ANL-95/40, Argonne National Laboratory (1995).
10) C. H. Adams, "Specifications for VARI3D - A Multidimensional Reactor Design Sensitivity Code," FRA-TM-74, Argonne National Laboratory (1975).
11) R. E. Alcouffe, F. W. Brinkley, D. R. Marr, R. D. O'Dell, "User's Guide for TWODANT: A Code Package for Two-Dimensional, Diffusion-Accelerated, Neutral-Particle Transport," LA-10049-M, Los Alamos National Laboratory (1990).
12) R. E. MacFarlane, "NJOY 99/2001: New Capabilities in Data Processing," presentation at the Workshop on Reactor Physics and Analysis Capabilities for Generation IV Nuclear Energy Systems, Argonne National Laboratory, Argonne, February 18-19, 2003.
13) R. N. Hill, "Coupled Neutron-Gamma Heating Calculations," private communication, Argonne National Laboratory, February 2, 1988.
14) W. S. Yang, "Fortran 77 Version of SE2-ANL," private communication, Argonne National Laboratory, March 3, 1993.
15) R. B. Vilim, "Reactor Hot Spot Analysis," FRA-TM-152, Argonne National Laboratory, August 1985.
16) J. E. Cahalan, A. M. Tentner, and E. E. Morris, "Advanced LMR Safety Analysis Capabilities in the SASSYS-1 and SAS4A Computer Codes," Proceedings of the International Topical Meeting on Advanced Reactors Safety, American Nuclear Society, Vol. 2, pp. 1038-1045, Pittsburgh, PA, April 17-21, 1994.